Information Sciences 569 (2021) 766–785

Contents lists available at ScienceDirect

Information Sciences

journal homepage: www.elsevier.com/locate/ins

Disturbance observer-based Takagi-Sugeno fuzzy control of a delay fractional-order hydraulic turbine governing system with elastic water hammer via frequency distributed model

Teng Ma [a,b], Bin Wang [a,b,*]

[a] Department of Electrical Engineering, College of Water Resources and Architectural Engineering, Northwest A&F University, Yangling 712100, China
[b] Key Laboratory of Agricultural Soil and Water Engineering in Arid and Semiarid Areas, Ministry of Education, Northwest A&F University, Yangling 712100, China

ARTICLE INFO

Article history:
Received 13 January 2021
Received in revised form 17 March 2021
Accepted 10 May 2021
Available online 13 May 2021

Keywords:
Takagi-Sugeno fuzzy control
Fractional-order hydraulic turbine governing system
Time delay
Frequency distributed model
Disturbance observer
Linear matrix inequality

ABSTRACT

The hydraulic turbine governing system (HTGS) is a core part of a hydropower station, and the dynamic characteristics of its transition process and stability under disturbances have been strong concerns for the stable operations of units. In this paper, a disturbance observer-based Takagi-Sugeno (T-S) fuzzy control (DOBFC) method using the frequency distributed model (FDM) is proposed to improve the anti-interference control performance of a delay fractional-order HTGS. First, a more practical mathematical model of a fractional-order HTGS considering both the mechanical time delay and an elastic water hammer is established, and then its fuzzy model is presented on the basis of the generalized T-S fuzzy rules. Second, the disturbance observer is constructed by utilizing the system state and disturbance information, and the output estimated value of the observer is input into the designed fuzzy state feedback controller to compensate for the effect of external disturbances on the system and achieve disturbance suppression. Third, by means of a new FDM transformation and the construction of a novel Lyapunov function, the stability condition and the parameter solving method of the controller are derived using the linear matrix inequality (LMI) technique. Finally, simulation results are given to verify the effectiveness of the proposed algorithm.

© 2021 Elsevier Inc. All rights reserved.

1. Introduction

As the world's largest source of renewable energy, hydropower has a rapid rate of development in many countries, plays an integral role in the clean energy transition and ensures that global low-carbon goals remain within reach [1,2]. In 2019, the global total hydropower installed capacity reached 1308 GW, and fifty countries added to their electricity generation capacity using hydropower stations [3,4]. With the rapid development of hydropower construction, the unit capacity has increased sharply, and its safe and stable operation has become a hot and difficult research topic. As the core component of starting up power plant dispatching units, connecting to the grid, increasing or decreasing loads and maintaining a stable output, the HTGS plays a vital role in the power station and power grid system safety [5,6]. Therefore, it is necessary to study the stability and efficient control scheme of HTGSs to ensure the long-term economic operations of hydropower stations and meet the demand of users.

* Corresponding author at: Department of Electrical Engineering, Northwest A&F University, Yangling 712100, Shaanxi, China.
E-mail address: binwang@nwsuaf.edu.cn (B. Wang).

https://doi.org/10.1016/j.ins.2021.05.013
0020-0255/© 2021 Elsevier Inc. All rights reserved.

At present, there are many studies on integer-order HTGS modeling and dynamic analysis; however, an HTGS essentially has complex nonlinear, multivariable coupling and nonminimum phase characteristics, and thus traditional integer-order calculus is not suitable for describing the physical properties of the governing system due to its limited nature [7–9]. Fractional calculus is a generalization of classical integrals and derivatives, and using fractional operators in engineering modeling is more accurate. The fractional derivative is a good tool to describe the memory characteristic of a hydraulic servo system and the viscoelasticity of a pressure pipeline flow [10,11]. Considering the influence of the servomotor action delay and water hammer in actual conditions, studying the control method of a fractional-order delay HTGS with an elastic water hammer is more in line with the practical engineering significance.

Due to the strong nonlinear characteristics of an HTGS, the relevant advanced control algorithms such as predictive control and sliding mode control are all based on nonlinear control theory, and the stability analysis and controller design process is complex [12,13]. In addition, the Lyapunov stability theory of an integer-order control system is difficult to apply to a fractional-order system, which makes the stability control of a nonlinear fractional-order HTGS more difficult [14,15]. The FDM provides a reference for the equivalent transformation of a fractional-order system into an integer-order time–frequency model since it can extend integer-order system control theory to a fractional-order system and has the advantages of simplifying the control of a fractional-order system [16,17]. As an effective method to solve the modeling and control problems of complex objects, fuzzy control has been received noticeable attention in control engineering [18–20]. Ref. [19] discusses a design of an optimized cascade fuzzy controller for the rotary inverted pendulum system. Ref. [20] proposes a stable fuzzy logic control of a general class of chaotic systems. As a hot spot of fuzzy control technology, T-S fuzzy control has the superiority of approximating nonlinear systems with arbitrary precision, and the analysis of a traditional linear system control method can be extended to nonlinear systems using the T-S fuzzy model. The controller design is simple and flexible with certain robustness [21]. Therefore, T-S fuzzy control as an effective control strategy is widely used in integer-order systems. Motivated by the prominent advantages of fuzzy control, the application of the generalized T-S fuzzy control method to fractional-order nonlinear systems has become the focus [22,23]. A robust fuzzy control method for fractional-order HTGS in the presence of random disturbances is investigated in [24]. Ref. [25] focuses on a fuzzy generalised predictive control method for a fractional-order HTGS; however, the combination of the FDM and T-S fuzzy control has not been reported. Moreover, the time lag will degrade the controllability of the system and even lead to instability [26–29]; accordingly, the T-S fuzzy control of a fractional-order HTGS with a mechanical time delay and an elastic water hammer is worth studying.

Furthermore, when the unit is switching in various working conditions, it is difficult to avoid the instability of the generating frequency caused by external stochastic disturbances such as load and frequency interference and mechanical vibration interference, thus affecting the quality and safety of the power supply [30]. At present, the fixed-parameter PID algorithm widely used in HTGSs cannot meet the high system response speed and accuracy requirements, and the steady-state error index is poor when the working conditions are disturbed, which may deteriorate the control performance [31,32]. Therefore, disturbance compensation should be considered in a control scheme designed for an HTGS. However, various external disturbances act on the internal states of the system; and due to their randomness and uncertainty, the technical complexity of the measurement methods and the limitations in the scope and economy of the applications, it is hard to directly use disturbance information to construct a controller to suppress interference [33]. By adding a disturbance observer to the governing system, the output observation value can be directly input into the control terminal to counteract the effect of external interference on the system. Currently, this method has been gradually applied to the fractional-order systems [34,35]. In general, both using the FDM to transform a fractional-order system and simplify stability analysis and T-S fuzzy control with a disturbance observer to improve control quality have potential advantages; therefore, it is desirable to know if the FDM can be introduced to DOBFC theory for a delay fractional-order HTGS with an elastic water hammer. To our best knowledge, there is no work relating to this problem. If this is feasible, how can the time delay be addressed? What would be the specific generalized delay T-S fuzzy model, the transformation from the fuzzy model to the FDM, the combined controller form, the stability condition and the detailed theoretical derivation? These are still open questions that require further study.

Inspired by the above analysis, some attractive advantages and contributions are derived from this work. The established six-dimensional fractional-order HTGS model takes the effects of an elastic water hammer and the time delay into account, which makes the model better fit the real production of hydropower stations. By extending the traditional T-S fuzzy concept, the corresponding generalized delay T-S fuzzy model is obtained. After constructing a nonlinear observer to identify and estimate the disturbance online, a DOBFC method is designed to realize disturbance suppression for the fuzzy delay fractional-order HTGS. To avoid the difficulty of selecting a suitable function and calculating the fractional derivative, the fractional-order delay HTGS based on the generalized fuzzy model is transformed into an equivalent FDM for the first time. On this basis, a novel monochromatic Lyapunov function is constructed, and the global asymptotic stability conditions of the closed-loop system are derived, providing a new approach for the stability analysis of a fractional-order HTGS. The main conclusion is realized by LMI and can be easily solved by a MATLAB toolbox. The simulations are used to verify the effectiveness and superiority of the proposed control scheme.

The remaining contents of this paper are structured as follows: In Section 2, the preliminaries are provided. The system description is presented in Section 3. The controller design and stability analysis are given in Section 4. In Section 5, numerical examples are simulated. Section 6 gives the conclusions.

2. Preliminaries

2.1. Fractional derivative and frequency distributed model

There are three kinds definitions commonly used for the fractional derivative. Caputo's definition has both theoretical research and clear physical significance, which makes it suitable for practical engineering applications. Consequently, Caputo's fractional derivative will be adopted in the modeling of an HTGS. The basic definition is briefly given below.

Definition 1 [36]:. *The fractional-order Caputo derivative of order $\alpha > 0$ for a continuous function $f(t)$ is defined as follows*:

$$\frac{C}{t_0}D_t^{\alpha}f(t) = t_0 I_t^{n-\alpha}\left(\frac{d}{dt}\right)^n f(t) = \begin{cases} \frac{1}{\Gamma(n-\alpha)}\int_{t_0}^{t}\frac{f^{(n)}(\tau)}{(t-\tau)^{\alpha-n+1}}d\tau, & n-1<\alpha<n \\ \frac{d^{\alpha}f(t)}{dt^{\alpha}}, & \alpha = n \end{cases} \tag{1}$$

where $n \in N$; $f^{(n)}(.)$ is the n-order derivative of function; $\Gamma(.)$ is the gamma function; ${}_{t_0}I_t^{n-\alpha}$ is the $n-\alpha$-order integral operator; and ${}_{t_0}^{C}D_t^{\alpha}$ denotes the α-order Caputo differential operator, which will be written as D^{α} for simplification in the following text.

To maintain the consistency of the fractional-order state space model, simplify the stability analysis and obtain the main result, the following lemma is introduced.

Lemma 1 [37]:. *Consider a nonlinear fractional-order system of the following form*:

$$D^{\alpha}X(t) = F(X(t)) \tag{2}$$

where $F(.)$ is a continuous differentiable function, and $X(t) \in R^n$ is the system state vector. The differential equation that is equivalent to system (2) can be expressed as:

$$\begin{cases} \frac{\partial\phi(\omega,\ t)}{\partial t} = -\omega\phi(\omega,t) + F(X(t)) \\ X(t) = \int_0^{\infty}\mu(\omega)\phi(\omega,\ t)d\omega \end{cases} \tag{3}$$

where ω is the elementary frequency; $\mu(\omega) = \frac{\sin(\alpha\pi)}{\pi}\omega^{-\alpha}(\alpha \in (0,\ 1))$ is the frequency weighting function of $\phi(\omega,\ t)$; and the state variable $\phi(\omega,\ t)$ replaces $X(t)$, which is infinite dimension-distributed and represents the true state of the system.

Remark 1:

Lemma 1 presents a method to transform a fractional-order system into an equivalent integer-order model based on the time–frequency domain conversion, and it avoids that the information of initial state X_0 cannot fully reflect the future behavior of the system. Through this lemma, the stability problem of a fractional-order system can be transformed into an integer-order one that is easy to solve.

The following lemma helps the derivation of the theorem.

Lemma 2 (Schur complement lemma [38]):

Given a real matrix $\Xi = \begin{bmatrix} \Xi_1 & \Xi_3 \\ \Xi_3^T & \Xi_2 \end{bmatrix}$ where $\Xi_1 \in R^{r\times r}$, $\Xi_1 = \Xi_1^T$ and $\Xi_2 = \Xi_2^T$, then the following two conditions are equivalent to $\Xi < 0$.

i. $\Xi_2 < 0$, $\Xi_1 - \Xi_3\Xi_2^{-1}\Xi_3^T < 0$.
ii. $\Xi_1 < 0$, $\Xi_2 - \Xi_3^T\Xi_1^{-1}\Xi_3 < 0$.

2.2. Generalized delay T-S fuzzy model

By extending the conventional integer-order fuzzy model theory, in the generalized T-S fuzzy method, the local linear representation of nonlinear fractional-order system is given by the IF-THEN rule. The linear subsystems can approximate or represent the original system via nonlinear fuzzy superposition according to different weights. When the state of the fractional-order system contains a constant time delay $\tau > 0$, the ith rule of the generalized delay T-S fuzzy model is expressed as follows:

Rule i: IF $\sigma_1(t)$ is M_{i1} and. . .and $\sigma_p(t)$ is M_{ip},

$$\text{THEN}\begin{cases} D^{\alpha}x(t) = A_i x(t) + A_{di}x(t-\tau) + B_i(u(t)+d(t)) \\ z(t) = C_i x(t) \end{cases} \tag{4}$$

where i = 1, 2, . . ., r; and the number of fuzzy rules is r. The measurable premise variables are $\sigma(t) = [\sigma_1(t),\ \sigma_2(t),\ ...,\ \sigma_p(t)]$, and they are independent of the control input. $M_{ij}(j = 1, 2, ..., p)$ denotes the fuzzy collection; $x(t) \in R^n$ is the state vector, the initial status of $x(t)$ is continuous over the interval $[-d, 0]$; $u(t) \in R^m$ and $z(t) \in R^p$are the control input and controlled output,

respectively; $d(t) \in L_2[0,+\infty)$ denotes the exogenous disturbance signal; and A_i, A_{di}, B_i and C_i are the known coefficient matrices of the appropriate dimensions.

According to fuzzy logic theory, the final defuzzified output of the generalized fractional-order time-delay T–S fuzzy model has the following form:

$$\begin{cases} D^{\alpha}x(t) = \sum_{i=1}^{r} h_i(\sigma(t))[A_i x(t) + A_{di}x(t-\tau) + B_i(u(t)+d(t))] \\ z(t) = \sum_{i=1}^{r} h_i(\sigma(t))C_i x(t) \end{cases} \tag{5}$$

where $h_i(\sigma(t)) = \psi_i(\sigma(t))/\sum_{i=1}^{r}\psi_i(\sigma(t))$, and $\psi_i(\sigma(t)) = \prod_{j=1}^{n} M_{ij}(\sigma_j(t))$. This holds for all $i \quad \sum_{i=1}^{r} h_i(\sigma(t)) = 1$ and $h_i(\sigma(t)) \in [0,1]$.

3. Fractional-order time-delay HTGS and its fuzzy model

Since the penstock and water have elastic properties, the dead zone of the main control valve and mechanical inertia of the relay displacement lead to time lag in the governing system. Based on the Caputo's definition in Section 2 and the model in Ref. [39], a six-order nonlinear fractional-order Francis HTGS with a mechanical time delay and an elastic water hammer is established:

$$\begin{cases} D^{\alpha}x_1 = x_2 \\ D^{\alpha}x_2 = x_3 \\ D^{\alpha}x_3 = -a_0x_1 - a_1x_2 - a_2x_3 + y(t-\tau) \\ D^{\alpha}\delta = w_0 w + u_1 \\ D^{\alpha}w = \frac{1}{T_{ab}}\left(m_t - \frac{E'_q V_s}{x'_{d\Sigma}}\sin\delta - \frac{V_s^2}{2}\frac{x'_{d\Sigma}-x_{q\Sigma}}{x'_{d\Sigma}x_{q\Sigma}}\sin 2\delta - Dw\right) + u_2 \\ D^{\alpha}y = -\frac{1}{T_y}y(t-\tau) + u_3 \end{cases} \tag{6}$$

where x_1, x_2 and x_3 represent intermediate state variables; $m_t = b_3 y(t-\tau) + (b_0 - a_0b_3)x_1 + (b_1 - a_1b_3)x_2 + (b_2 - a_2b_3)x_3$; $b_0 = \frac{24e_y}{e_{qh}h_w T_r^3}$; $b_1 = -\frac{24ee_y}{e_{qh}T_r^2}$; $b_2 = \frac{3e_y}{e_{qh}h_w T_r}$; $b_3 = -\frac{ee_y}{e_{qh}}$; $a_0 = \frac{24}{e_{qh}h_w T_r^3}$; $a_1 = \frac{24}{T_r^2}$ and $a_2 = \frac{3}{e_{qh}h_w T_r}$. Variables δ, w and y are dimensionless and represent the deviations of the generator rotor angle, the generator rotor speed, and the incremental deviation of the master servomotor stroke, respectively. In the hydraulic turbine and penstock system, h_w is the characteristic parameter of the penstock, and T_r is the water hammer inertia time constant. e_{qh}, e_y and e are the flow on the water head transfer coefficient, master servomotor stroke transfer coefficient and self-adjusting coefficient, respectively. In a synchronous generator system, D is the damping coefficient, the rated angular speed $w_0 = 2\pi f_0$ and $f_0 = 50$ Hz. T_{ab} is the inertia time constant of the unit mechanical part. E'_q represents the q-axis transient voltage, V_s is the bus voltage, and $x'_{d\sum}$ and $x_{q\sum}$ are the reactances of the d-axis and q-axis, respectively. In a hydraulic servo system, discrete time delay $\tau > 0$, and T_y denotes the response time constant of the engager relay. u_1, u_2 and u_3 are the control inputs from the designed controller. For $t \in [0,\tau]$, $D^{\alpha}y = D^{\alpha}y(t) = y_0$. The system order $\alpha \in (0,\ 1)$.

To facilitate the mathematical analysis, select state vector $x(t) = [x_1(t), x_2(t), x_3(t), \delta(t), w(t), y(t)]^T = [x_1(t), x_2(t), x_3(t), x_4(t), x_5(t), x_6(t)]^T$. Considering that external disturbances affect the system, the state equation of system (6) can then be obtained as follows:

$$\begin{cases} D^{\alpha}x(t) = Af(x(t)) + A_d x(t-\tau) + B(u(t)+d(t)) \\ z(t) = Cx(t) \end{cases} \tag{7}$$

where

$$A = \begin{bmatrix} 0 & 1 & 0 & 0 & 0 & 0 \\ 0 & 0 & 1 & 0 & 0 & 0 \\ -a_0 & -a_1 & -a_2 & 0 & 0 & 0 \\ 0 & 0 & 0 & 0 & w_0 & 0 \\ \frac{b_0-a_0b_3}{T_{ab}} & \frac{b_1-a_1b_3}{T_{ab}} & \frac{b_2-a_2b_3}{T_{ab}} & \frac{1}{T_{ab}} & -\frac{D}{T_{ab}} & 0 \\ 0 & 0 & 0 & 0 & 0 & 0 \end{bmatrix} \quad A_d = \begin{bmatrix} 0 & 0 & 0 & 0 & 0 & 0 \\ 0 & 0 & 0 & 0 & 0 & 0 \\ 0 & 0 & 0 & 0 & 0 & 1 \\ 0 & 0 & 0 & 0 & 0 & 0 \\ 0 & 0 & 0 & 0 & 0 & -\frac{ee_y}{e_{qh}T_{ab}} \\ 0 & 0 & 0 & 0 & 0 & -\frac{1}{T_y} \end{bmatrix} \text{ and}$$

$$f(x(t)) = \begin{bmatrix} x_1(t) \\ x_2(t) \\ x_3(t) \\ -\frac{E'_q V_s}{x'_{d\Sigma}}\sin x_4(t) - \frac{V_s^2}{2}\frac{x'_{d\Sigma}-x_{q\Sigma}}{x'_{d\Sigma}x_{q\Sigma}}\sin 2x_4(t) \\ x_5(t) \\ x_6(t) \end{bmatrix}$$

$f(x(t))$ represents the nonlinear state vector without a time delay; A is the corresponding coefficient matrix; A_d is the coefficient matrix of the time-delay state vector; $u(t) = [u_1(t),\ u_2(t),\ u_3(t)]^T$ and $z(t)$ denote the control input and controlled output of the governing system, respectively; and B and C are appropriate coefficient matrices of the input and output vectors; respectively.

The disturbance $d(t)$ in system (7) is derived from the following exogenous system:

$$\begin{cases} D^{\alpha}\xi(t) = W\xi(t) \\ d(t) = V\xi(t) \end{cases} \tag{8}$$

where $\xi(t)$ represents the system state vector. The bounded $d(t)$ results from the external stochastic excitation and uncertainties, and it satisfies the following: for any $T > 0$, $\int_0^T d^{\mathrm{T}}(t)d(t)dt < +\infty$. W and V are known proper matrices. In general, it is assumed that system (8) is neutral stable, which indicates that $d(t)$ is continuously applied to system (7).

Before designing the control method, the nonlinear term of the delay fractional-order system (7) should be processed to obtain the corresponding T-S fuzzy model. Considering the boundedness of chaotic motion, select $x_4(t) \in [-\rho, \rho]$, where ρ is a constant. Construct the related fuzzy set function with $x_4(t)$ as the antecedent condition. The following two fuzzy rules are applied to system (7):

Rule 1: IF $x_4(t)$ is $M_{11}(x_4(t))$ (near 0)

THEN $\begin{cases} D^{\alpha}x(t) = A_1x(t) + A_{d1}x(t-\tau) + B_1(u(t)+d(t)) \\ z(t) = C_1x(t) \end{cases}$

Rule 2: IF $x_4(t)$ is $M_{21}(x_4(t))$ (near $\pm\rho$)

THEN $\begin{cases} D^{\alpha}x(t) = A_2x(t) + A_{d2}x(t-\tau) + B_2(u(t)+d(t)) \\ z(t) = C_2x(t) \end{cases}$ where A_1, A_2, A_{d1}, A_{d2}, C_1 and C_2 are the real constant matrices; $A_i(i = 1, 2)$ is obtained by using the local approximation modeling method of the Maclaurin series expansion to handle the nonlinear term; and B_1 and B_2 are the coefficient matrices of the input with proper dimension. The membership functions are presented as: $M_{11}(x_4(t)) = \frac{1}{2}\left(1 + \frac{x_4(t)}{\rho}\right)$ and $M_{21}(x_4(t)) = \frac{1}{2}\left(1 - \frac{x_4(t)}{\rho}\right)$.

By multiplying the two local fractional-order linear subsystems by their weights to achieve fuzzy superposition, the global T-S fuzzy model of a delay fractional-order HTGS can be formed as follows:

$$\begin{cases} D^{\alpha}x(t) = \sum_{i=1}^{2} h_i(\sigma(t))[A_ix(t) + A_{di}x(t-\tau) + B_i(u(t)+d(t))] \\ z(t) = \sum_{i=1}^{2} h_i(\sigma(t))C_ix(t) \end{cases} \tag{9}$$

For the convenience of the analysis, it can be abbreviated as:

$$\begin{cases} D^{\alpha}x(t) = A_hx(t) + A_{hd}x(t-\tau) + B_h(u(t)+d(t)) \\ z(t) = C_hx(t) \end{cases} \tag{10}$$

where $A_h = \sum_{i=1}^{2} h_i(\sigma(t))A_i$, $A_{hd} = \sum_{i=1}^{2} h_i(\sigma(t))A_{di}$, $B_h = \sum_{i=1}^{2} h_i(\sigma(t))B_i$ and $C_h = \sum_{i=1}^{2} h_i(\sigma(t))C_i$.

4. Controller design and stability analysis

According to the fractional-order properties and fuzzy inference rules in Section 2, a DOBFC scheme is proposed by combining the Lyapunov method and FDM conversion in this section. A nonlinear observer is established in the fuzzy governing system, and the reconstructed disturbances are introduced into the designed fuzzy state feedback controller to eliminate the influence of external interference on the system and the unit. The structural diagram of the closed-loop system is shown in Fig. 1.

To estimate $d(t)$ in system (7), the following disturbance observer is constructed:

$$\begin{cases} D^{\alpha}\varsigma(t) = (W_h + L_hB_hV)\hat{\xi}(t) + L_h[A_hx(t) + A_{hd}x(t-\tau) + B_hu(t)] \\ \hat{\xi}(t) = \varsigma(t) - L_hx(t) \\ \hat{d}(t) = V\hat{\xi}(t) \end{cases} \tag{11}$$

where $\varsigma(t)$ denotes the auxiliary vector as an internal state of the observer, $\hat{\xi}(t)$ is the estimation of $\xi(t)$ defined in (8), $\hat{d}(t)$ is the observed disturbance, $W_h = \sum_{i=1}^{2} h_i(\sigma(t))W_i$, $L_h = \sum_{j=1}^{2} h_i(\sigma(t))L_j$, $W_i(i = 1, 2)$ is the known appropriate matrix and $L_j(j = 1, 2)$ is the observer gain matrix to be determined. From (8), (10) and (11), it can be concluded that:

$$\begin{aligned} D^{\alpha}\hat{\xi}(t) &= D^{\alpha}\varsigma(t) - L_hD^{\alpha}x(t) \\ &= (W_h + L_hB_hV)\hat{\xi}(t) + L_h[A_hx(t) + A_{hd}x(t-\tau) + B_hu(t)] \\ &\quad -L_h[A_hx(t) + A_{hd}x(t-\tau) + B_h(u(t)+d(t))] \\ &= (W_h + L_hB_hV)\hat{\xi}(t) - L_hB_hV\xi(t) \end{aligned} \tag{12}$$

Due to the lack of predictability of the external stochastic disturbance, the disturbance error in the observer should be estimated in order to ensure the optimal control performance of the closed-loop control system. Therefore, $e(t) = \xi(t) - \hat{\xi}(t)$ is defined as the exogenous system state observation error, and its dynamic characteristic satisfies:

$$D^{\alpha}e(t) = D^{\alpha}\xi(t) - D^{\alpha}\hat{\xi}(t) = (W_h + L_hB_hV)e(t) \tag{13}$$

It is assumed that the states of the governing system are available for measurement. Then, the proposed controller for system (10) is given as follows:

$$u(t) = u_k(t) + u_z(t) \tag{14}$$

where $u_z(t) = -\hat{d}(t)$.

The design of fuzzy controller $u_k(t)$ is based on the parallel distributed compensation (PDC) theory. Based on the fuzzy theory of Section 2 and the fuzzification method of the HTGS in Section 3, the memoryless state feedback control law could be obtained by adopting two IF-THEN rules:

Rule 1: IF $x_4(t)$ is $M_{11}(x_4(t))$ (near 0), THEN $u_k(t) = K_1x(t)$.

Rule 2: IF $x_4(t)$ is $M_{21}(x_4(t))$ (near $\pm\rho$), THEN $u_k(t) = K_2x(t)$.where $K_i(i = 1, 2)$ is the gain matrix of the ith rule to be designed. The final form of the fuzzy controller is:

$$u_k(t) = \sum_{i=1}^{2} h_i(\sigma(t))K_ix(t) \tag{15}$$

Substituting (14) into (10), the following closed-loop governing system with an error estimation is derived below:

$$\begin{aligned} D^{\alpha}x(t) &= A_hx(t) + A_{hd}x(t-\tau) + B_h(u(t) + d(t)) \\ &= \sum_{i=1}^{2} h_i(\sigma(t))[A_ix(t) + A_{di}x(t-\tau) + B_iVe(t)] \\ &\quad + \sum_{i=1}^{2} h_i(\sigma(t))\left[B_i \sum_{j=1}^{2} h_j(\sigma(t))K_jx(t)\right] \\ &= \sum_{i=1}^{2}\sum_{j=1}^{2} h_i(\sigma(t))h_j(\sigma(t))\left[(A_i + B_iK_j)x(t) + A_{di}x(t-\tau) + B_iVe(t)\right] \end{aligned} \tag{16}$$

To reproduce the states of system (16) for further analysis, we let:

$$\varphi(t) = \left[x^T(t)\ e^T(t)\right]^T \tag{17}$$

Augmenting equations (13), (16) and (17), the general state-space equation of the closed-loop composite system is given as follows:

$$D^{\alpha}\varphi(t) = A_z\varphi(t) + A_{zd}\varphi(t-\tau) \tag{18}$$

where $A_z = \sum_{i=1}^{2}\sum_{j=1}^{2} h_i(\sigma(t))h_j(\sigma(t))\begin{bmatrix} A_i + B_iK_j & B_iV \\ 0 & W_i + L_jB_iV \end{bmatrix}$, and $A_{zd} = \sum_{i=1}^{2} h_i(\sigma(t))\begin{bmatrix} A_{di} & 0 \\ 0 & 0 \end{bmatrix}$.

Now, the design of the control method can be realized by analyzing the stabilization problem of a fractional-order time-delay system. Next, the LMI-based asymptotic stability condition of system (18) under control law (14) is derived in the following theorems.

Theorem 1:. *The composite fractional-order system (18) with a time delay can achieve asymptotic stability if positive definite symmetric matrices P and Q exist, making the following inequality hold.*

$$\begin{bmatrix} A_z^TP + PA_z + Q & PA_{zd} \\ * & -Q \end{bmatrix} < 0 \tag{19}$$

"*" represents the transpose of the matrix.

Proof:. *By applying the theory in Lemma* 1, *system (18) can be equally expressed as the following integer-order model.*

$$\begin{cases} \frac{\partial Z(\omega,t)}{\partial t} = -\omega Z(\omega,t) + A_z\varphi(t) + A_{zd}\varphi(t-\tau) \\ \varphi(t) = \int_0^{\infty} \mu(\omega)Z(\omega,t)d\omega \end{cases} \tag{20}$$

Auxiliary function $Z(\omega, t)$ is defined in both the time and frequency domains, First, construct an elementary monochromatic Lyapunov function $v(\omega, t) = Z^T(\omega, t)PZ(\omega, t)$ of the internal state variable $Z(\omega, t)$, and then integrate the product of $v(\omega, t)$ and weighting function $\mu(\omega)$ in the infinite frequency domain, namely, the first Lyapunov function is defined as:

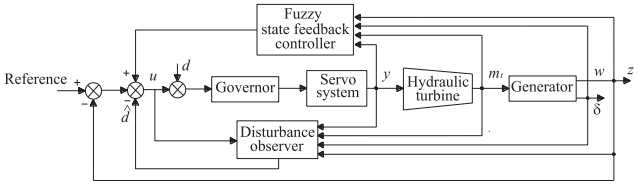

Fig. 1. Block diagram of the disturbance observer-based fractional-order delay HTGS.

$$V_1(t) = \int_0^\infty \mu(\omega) v(\omega,t) d\omega = \int_0^\infty \mu(\omega) Z^T(\omega,t) P Z(\omega,t) d\omega \tag{21}$$

where symmetric square matrix P is positive definite. Accordingly, $v(\omega,t)$ is positive. Meanwhile, for all ω, $\mu(\omega) > 0$. Therefore, $V_1(t)$ is a positive function.

The derivative of $V_1(t)$ is taken with respect to time along the trajectories of (18). This yields:

$$\begin{aligned}
\dot{V}_1(t) &= \int_0^\infty \mu(\omega) \tfrac{\partial}{\partial t} \left(Z^T(\omega,t) P Z(\omega,t) \right) d\omega \\
&= \int_0^\infty \mu(\omega) \left(\tfrac{\partial Z^T(\omega,t)}{\partial t} P Z(\omega,t) + Z^T(\omega,t) P \tfrac{\partial Z(\omega,t)}{\partial t} \right) d\omega \\
&= \int_0^\infty \mu(\omega) \left[-\omega Z^T(\omega,t) + \varphi^T(t) A_z^T + \varphi^T(t-\tau) A_{zd}^T \right] P Z(\omega,t) d\omega \\
&+ \int_0^\infty \mu(\omega) Z^T(\omega,t) P [-\omega Z(\omega,t) + A_z \varphi(t) + A_{zd} \varphi(t-\tau)] d\omega \\
&= -2 \int_0^\infty \omega \mu(\omega) Z^T(\omega,t) P Z(\omega,t) d\omega + \int_0^\infty \mu(\omega) \left(\varphi^T(t) A_z^T + \varphi^T(t-\tau) A_{zd}^T \right) P Z(\omega,t) d\omega \\
&+ \int_0^\infty \mu(\omega) Z^T(\omega,t) P (A_z \varphi(t) + A_{zd} \varphi(t-\tau)) d\omega \\
&= -2 \int_0^\infty \omega \mu(\omega) Z^T(\omega,t) P Z(\omega,t) d\omega + \left(\varphi^T(t) A_z^T + \varphi^T(t-\tau) A_{zd}^T \right) P \int_0^\infty \mu(\omega) Z(\omega,t) d\omega \\
&+ \left(\int_0^\infty \mu(\omega) Z^T(\omega,t) d\omega \right) P (A_z \varphi(t) + A_{zd} \varphi(t-\tau)) \\
&= -2 \int_0^\infty \omega \mu(\omega) Z^T(\omega,t) P Z(\omega,t) d\omega + 2 \varphi^T(t) P A_z \varphi(t) + 2 \varphi^T(t) P A_{zd} \varphi(t-\tau)
\end{aligned} \tag{22}$$

Subsequently, the second Lyapunov candidate function is defined:

$$V_2(t) = \int_{t-\tau}^t \varphi^T(s) Q \varphi(s) ds \tag{23}$$

where Q is a symmetric positive definite matrix, the time derivative of $V_2(t)$ along system (18) is obtained:

$$\dot{V}_2(t) = \varphi^T(t) Q \varphi(t) - \varphi^T(t-\tau) Q \varphi(t-\tau) \tag{24}$$

The final global Lyapunov function of system (18) is the sum of $V_1(t)$ and $V_2(t)$, which is denoted as $V(t) = V_1(t) + V_2(t)$. From (22) and (24), one obtains:

$$\begin{aligned}
\dot{V}(t) &= -2 \int_0^\infty \omega \mu(\omega) Z^T(\omega,t) P Z(\omega,t) d\omega + 2 \varphi^T(t) P A_z \varphi(t) + 2 \varphi^T(t) P A_{zd} \varphi(t-\tau) \\
&+ \varphi^T(t) Q \varphi(t) - \varphi^T(t-\tau) Q \varphi(t-\tau)
\end{aligned} \tag{25}$$

The inequality derived to satisfy that $\dot{V}(t)$ is nonpositive, thus ensuring system (18) is asymptotically stable around the equilibrium point $Z(\omega,t) = 0$, is as follows:

$$\begin{aligned}
&2 \varphi^T(t) P A_z \varphi(t) + 2 \varphi^T(t) P A_{zd} \varphi(t-\tau) + \varphi^T(t) Q \varphi(t) - \varphi^T(t-\tau) Q \varphi(t-\tau) \\
&= \varphi^T(t) \left(A_z^T P + P A_z + Q \right) \varphi(t) - \varphi^T(t-\tau) Q \varphi(t-\tau) + \varphi^T(t) P A_{zd} \varphi(t-\tau) \\
&+ \varphi^T(t-\tau) A_{zd}^T P \varphi(t) \leqslant 0
\end{aligned} \tag{26}$$

This is further treated by applying the Schur complement to obtain the following more practical condition:

$$\Xi^T \begin{bmatrix} A_z^T P + P A_z + Q & P A_{zd} \\ * & -Q \end{bmatrix} \Xi < 0 \tag{27}$$

where $\Xi = \begin{bmatrix} \varphi(t) \\ \varphi(t-\tau) \end{bmatrix}$.

Therefore, the existence of inequality (19) is a sufficient stability condition of system (18) under the control law (14). The proof is completed.

Remark 2:. *The Lyapunov stability theory of fractional-order systems with time delay [15,40,41] indicates that it is difficult to find the appropriate positive definite function and calculate the fractional derivative. Moreover, due to the influence of actual environment, when the differential order of the system is perturbed, the derivative of the constructed function will change significantly, and the original stability criteria will be invalid. The DOBFC studied in this paper constructs an appropriate Lyapunov function with the help of FDM, which avoids some difficulties in the stability analysis of fractional-order time-delay systems.*

The study object of the stability analysis method proposed above is the whole composite system. To solve the gain parameters of the feedback controller and the observer conveniently, the following LMIs are further acquired on the basis of Theorem 1.

Theorem 2:. *The composite fractional-order system (18) with a time delay can achieve asymptotic stability under the control law (14) if there are symmetric positive definite matrices P_1, P_2, $\bar{Q}_1$ and $\bar{Q}_2$, nonsingular matrix $X > 0$, and appropriate matrices H_j, $Y_j (j = 1, 2)$, making the following LMIs hold*:

$$\begin{bmatrix} \Omega & \Psi & Q \\ * & -Q & 0 \\ * & * & -Q \end{bmatrix} < 0 (i = 1, 2) \tag{28}$$

$$\begin{bmatrix} \tilde{\Omega} & \tilde{\Psi} & 2Q \\ * & -2Q & 0 \\ * & * & -2Q \end{bmatrix} < 0 (1 \leqslant i \neq j \leqslant 2) \tag{29}$$

where

$$\Omega = \begin{bmatrix} XA_i^T + A_iX + Y_i^TB_i^T + B_iY_iB_iV \\ *P_2W_i + W_i^TP_2 + V^TB_i^TH_i^T + H_iB_iV \end{bmatrix}$$

$$\Psi = \begin{bmatrix} A_{di}X0 \\ 00 \end{bmatrix}$$

$$\tilde{\Omega} = \begin{bmatrix} XA_i^T + A_iX + Y_j^TB_i^T + B_iY_j & B_iV + B_jV + XA_j^T + A_jX + Y_i^TB_j^T + B_jY_i \\ * & P_2W_i + W_i^TP_2 + V^TB_i^TH_j^T + H_jB_iV + P_2W_j + W_j^TP_2 + V^TB_j^TH_i^T + H_iB_jV \end{bmatrix}$$

$$\tilde{\Psi} = \begin{bmatrix} A_{di}X + A_{dj}X & 0 \\ 0 & 0 \end{bmatrix}$$

In addition, the gain matrices of the controller and observer are $K_j = Y_jX^{-1}$ and $L_j = P_2^{-1}H_j$, respectively.

Proof:. *Similar to Lemma 2, the following inequality equivalent to (19) is obtained.*

$$\begin{bmatrix} A_z^TP + PA_zPA_{zd} & Q \\ * & -Q0 \\ * & *-Q \end{bmatrix} < 0 \tag{30}$$

Assume $P = diag(P_1, P_2)$ and $Q = diag(Q_1, Q_2)$. Based on the definitions of matrices A_z and A_{zd}, (30) can be rewritten as:

$$\sum_{i=1}^{2}\sum_{j=1}^{2} h_i(\sigma(t))h_j(\sigma(t)) \begin{bmatrix} A_i^TP_1 + P_1A_i + K_j^TB_i^TP_1 + P_1B_iK_j \\ * \\ * \\ * \\ * \\ * \end{bmatrix}$$

$$\begin{matrix} P_1B_iVP_1A_{di}0Q_10 \\ W_i^TP_2+P_2W_i+V^TB_i^TL_j^TP_2+P_2L_jB_iV000Q_2 \\ *\ -Q_1\ 000 \\ **-Q_200 \\ ***-Q_1\ 0 \\ ****-Q_2 \end{matrix} < 0$$

$$=\sum_{i=1}^{2}h_i^2(\sigma(t))\ G_{ii}+\sum_{i=1}^{2}\sum_{j=1}^{2}h_i(\sigma(t))h_j(\sigma(t))\left(G_{ij}+G_{ji}\right)<0 \tag{31}$$

where

$$G_{ij}=\begin{bmatrix} A_i^TP_1+P_1A_i+K_j^TB_i^TP_1+P_1B_iK_j \\ * \\ * \\ * \\ * \\ * \end{bmatrix}$$

$$\begin{matrix} P_1B_iVP_1A_{di}0Q_10 \\ W_i^TP_2+P_2W_i+V^TB_i^TL_j^TP_2+P_2L_jB_iV000Q_2 \\ *-Q_1000 \\ **-Q_200 \\ ***-Q_10 \\ ****-Q_2 \end{matrix} \quad (1\leqslant i\neq j\leqslant 2)$$

Since $\sum_{i=1}^{2}\sum_{j=1}^{2}h_i(\sigma(t))h_j(\sigma(t))=1$, $h_i(\sigma(t))\geqslant 0$ and $h_j(\sigma(t))\geqslant 0$, that is, (31) can be solved by the following two equivalent inequalities:

$$G_{ii}<0\,(i=1,2) \tag{32}$$

$$G_{ij}+G_{ji}<0\,(1\leqslant i\neq j\leqslant 2) \tag{33}$$

Further treatment is needed to make (32) and (33) feasible; therefore, both sides of inequality (32) are pre- and postmultiplied by an auxiliary matrix $diag\left(P_1^{-1},I,P_1^{-1},I,P_1^{-1},I\right)$, and $X=P_1^{-1}$, $Y_i=K_iP_1^{-1}$, $H_i=P_2L_i$, $\bar{Q}_1=P_1^{-1}Q_1P_1^{-1}$ and $\bar{Q}_2=Q_2$. This obviously shows that inequalities (32) and (28) are equivalent.

Since

$$G_{ij}+G_{ji}=\begin{bmatrix} \Delta_1P_1(B_i+B_j)V\ P_1(A_{di}+A_{dj})02Q_1\ 0 \\ *\Delta_2000\Delta_2 \\ **-2Q_1000 \\ ***-2Q_2\ 00 \\ ****-2Q_10 \\ *****-2Q_2 \end{bmatrix}<0,\ (1\leqslant i\neq j\leqslant 2) \tag{34}$$

where $\Delta_1=A_i^TP_1+P_1A_i+K_j^TB_i^TP_1+P_1B_iK_j+A_j^TP_1+P_1A_j+K_i^TB_j^TP_1+P_1B_jK_i$ and

$$\Delta_2=W_i^TP_2+P_2W_i+V^TB_i^TL_j^TP_2+P_2L_jB_iV+W_j^TP_2+P_2W_j+V^TB_j^TL_i^TP_2+P_2L_iB_jV$$

Analogously, both sides of (33) are pre- and postmultiplied by $diag\left(P_1^{-1},I,P_1^{-1},I,P_1^{-1},I\right)$. Then, the obtained equivalent matrix inequality (29) is easy to solve. Theorem 2 is proved.

Feedback control gains K_1 and K_2 and observer gains L_1 and L_2 can be obtained by using MATLAB to solve conditions (28) and (29).

5. Simulation results analysis

This section presents numerical simulations to validate the effectiveness of the designed control scheme applied to the fractional-order HTGS. According to the hydroelectric unit experiment and calculations, the following system parameters are determined in this paper.

$w_0 = 314$ rad/s, $T_{ab} = 8.0$ $D = 0.5$ $E'_q = 1.35$ $x'_{d\sum} = 1.15$ $x_{q\sum} = 1.474$ $V_s = 1.0$ $T_y = 0.1$ $e = 0.7$ $e_{qh} = 0.5$ $e_y = 1.0$, $T_r = 1.0$ $h_w = 2.0$ and $\rho = 4$. The relevant coefficient matrices are set as:$B = B_i(i = 1, 2)$ = [0 00; 0 00; 0 00; 100; 0 10; 0 01] $W = V = C = I_{3\times3}$, $W_i(i = 1, 2) = I_{3\times3}$and $C_i(i = 1, 2) = I_{3\times3}$. According to Section. 3 and the controller design method in Section. 4, the subsystem coefficient matrices and the gain matrix parameters solved are shown below:

$$A_1 = \begin{bmatrix} 010000 \\ 001000 \\ -24-24-3000 \\ 00003140 \\ 7.200.9\frac{116}{855}-0.06250 \\ 000000 \end{bmatrix} A_2 = \begin{bmatrix} 010000 \\ 001000 \\ -24-24-3000 \\ 00003140 \\ 7.200.9\frac{2858}{1033}-0.06250 \\ 000000 \end{bmatrix}$$

$$A_{d1} = A_{d2} = \begin{bmatrix} 000000 \\ 000000 \\ 000001 \\ 000000 \\ 00000-0.175 \\ 00000-10 \end{bmatrix}$$

$$K_1 = \begin{bmatrix} 0.00940.0034 & -0.2119 & -9.3270 & -157.5028 & 0.0603 \\ -6.4301 & -0.0310 & -0.7939 & -157.4898 & -9.10580.0349 \\ -2.0080 & -2.02221.98661.4774 & -0.3522 & -25.8593 \end{bmatrix}$$

$$K_2 = \begin{bmatrix} 0.00950.0034 & -0.2136 & -9.3270 & -157.04530.0732 \\ -6.4297 & -0.0309 & -0.8043 & -157.0236 & -9.1047\ 0.1578 \\ -2.0080 & -2.02221.98671.4769 & -0.3993 & -25.8605 \end{bmatrix}$$

$$L_1 = \begin{bmatrix} -9.5283 & -29.36919.387118.5425\ 75.2911 & -3.0387 \\ 28.3691 & -9.528310.58060.9130 & -35.0090 & -185.2046 \\ 14.850628.2480 & -3.3178\ 2.9739 & -107.2577 & -36.8286 \end{bmatrix}$$

$$L_2 = \begin{bmatrix} -9.5283\ 39.66518.9416 & -1.648412.8088 & -20.3104 \\ -40.6651 & -9.528336.0380\ 14.19627.0278 & -152.7111 \\ 16.83730.1991 & -8.0356 & -0.3294 & -18.206317.0228 \end{bmatrix}$$

The above controller parameters were obtained by using feasp in LMI toolbox to solve an auxiliary convex optimization problem. The toolbox adopts the projection algorithm, which is more efficient. To avoid producing large numerical solutions, speed up the calculation process and improve the numerical stability, the maximum iteration and the feasible region radius in the parameter calculation process are set as 100 and $R = 10^9$. For the CPU model of Intel(R) Core(TM) i7 CPU @ 3.10 GHz, the total time of running the program once is 3.573 s. The temporary memory needed in one feasp execution is 90.5275 kB, which has low time and space complexity.

Considering the uncertain fluctuation of the power grid load and shafting vibration, the random disturbances are set as $0.1\sin(5t) + 0.01\text{rand}(1)$; and the initial values of the disturbance observer and the system state are set as 0.1 and 0.01, respectively. This paper assumes that when the state variables respond to the equilibrium point, the hydrogenerator unit runs to the stable rated working condition, so the reference value of the stable system state output is set as 0. The following different cases are considered for controlling the fractional-order hydroelectric plant.

5.1. Case 1: Precontrol system characteristics

When there is no control input signal, the state trajectories of the governing system operating after grid connection are shown in Fig. 2. It is clear that the system states oscillate irregularly for a long time, which makes it difficult for the hydraulic servo system to control the servomotor to maintain the fixed guide vane opening; therefore, unit scheduling is difficult. From

the engineering perspective, the uncontrolled state is not conducive to the overall safe and stable operation of the system. In addition, the simulation curve shown in Fig. 3 demonstrates that the output of the observer cannot track the external disturbance accurately in the absence of control, that is, the open-loop control system cannot achieve interference suppression.

5.2. Case 2: Controlled system characteristics

The operating characteristics of the controlled fractional-order HTGS are studied under two conditions: no disturbance observations are introduced into controller (15), and disturbance compensation is considered when controller (14) is reconstructed. As seen from the comparison in Fig. 4, under the action of control law (15), the system can reach the expected stable response range in a short time. Compared with the uncontrolled HTGS, state feedback controller (15) is practical and effective. However, due to the lack of real-time suppression of external disturbances during the control process, there will be a small periodic oscillation near the steady state in which the amplitude of generator power angle can reach 6×10^{-3}; moreover, such oscillation in the stroke of the servomotor will also affect the flow regulation, which will degrade the power supply quality. For system (16) in which a disturbance observer is constructed, first, Fig. 5 shows that the observer designed in the controlled system can quickly and accurately identify and track the external disturbance, and the tracking error can be limited within 1% after 1.5 s. The estimation error is satisfactory, so the disturbance information can be input into the feedback controller correctly and timely to compensate for the impact of external disturbance in real time online. As shown in Fig. 4, controller (14) can ensure that the generator rotor power angle and angular speed and the servo motor stroke are strictly stabilized at the expected steady-state value, and the maximum deviations generated by the rotor power angle and guide vane opening are reduced by 0.004 and 0.013, respectively. The angular speed can be restored to the rating faster after grid connection and thus maintain a stable power supply frequency. These excellent performances can effectively realize the smooth opening and closing of the guide vane to balance the torque when the unit encounters a random fluctuation of the power grid load and other interference to reduce the frequency fluctuation as far as possible and meet the practical engineering requirements.

Fig. 6 shows that during the transition process, the control inputs corresponding to the generator power angle, rotor angular velocity and guide vane opening tend to a stable interval after a short period of oscillation, which indicates that the governing system has entered a relatively stable operating state under the controller's function. For the controller without disturbance information, the final output is kept at 0. The disturbances present in an HTGS are usually a collection of electrical and mechanical disturbances. The output of the controller based on the observer reflects the time-varying disturbance existing in the system after the transition stage, that is, the control signal can be adjusted at any time to govern the

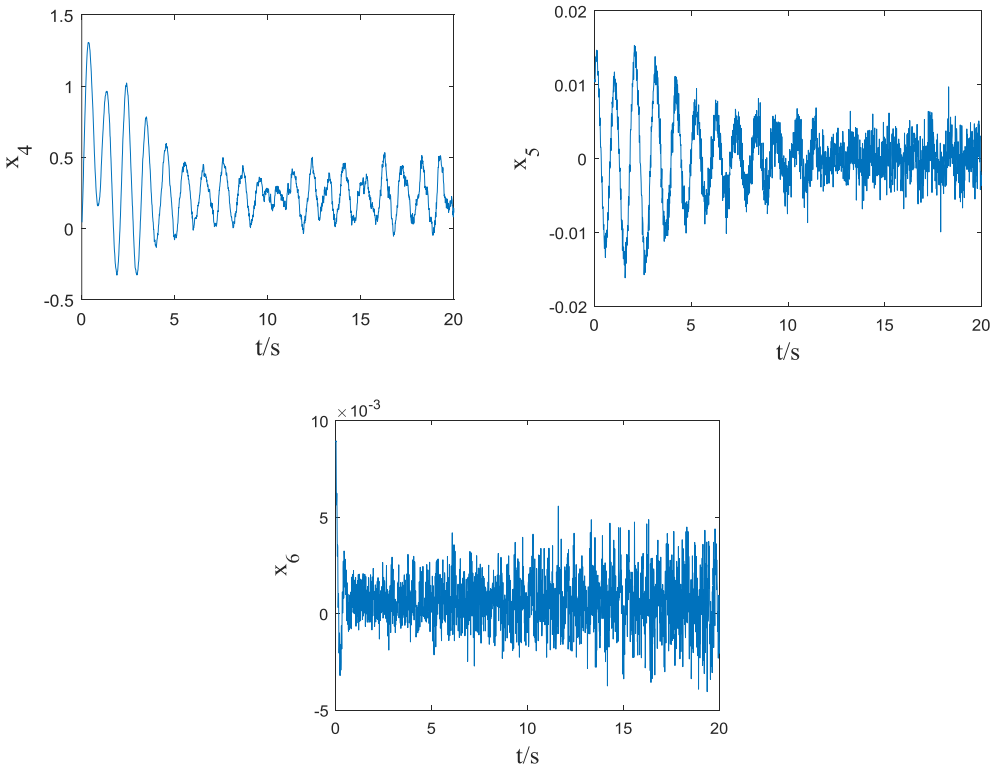

Fig. 2. State trajectories of the uncontrolled fractional-order HTGS.

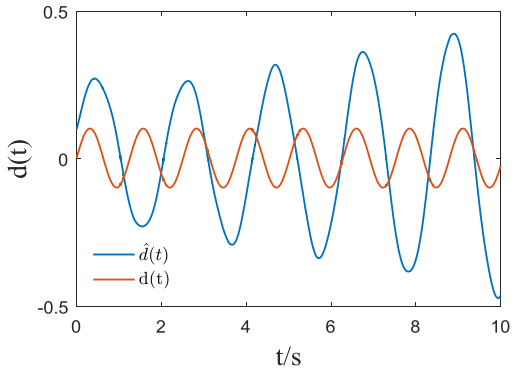

Fig. 3. Disturbance and its estimated value of the uncontrolled fractional-order HTGS.

system to provide good dynamic performance with a short adjustment time and small overshoot and ensure better steady-state performance.

5.3. Case 3: Effects of a time delay

Consider that the mechanical inertia of an actuator causes the water guide system to be unable to track the target value and adjust the flow quickly according to the control signal in real time. Therefore, it is necessary to verify the validity of the DOBFC to varying degrees of relay delay. The upper limit of the delay constant is 0.2 s, and the output response curves under four different time lags are shown in Fig. 7. Generally, when the delay increases, the system control quality will deteriorate, and the change of the delay has a greater impact on the control effect of the rotor angular speed and servomotor stroke. Specifically, when τ increases from 0.05 s to 0.2 s, the difference between the trough and the second peak of the guide vane opening response curve increases by 0.0044, 0.0058 and 0.0069, respectively; and the settle time increases by 0.18 s, 0.25 s and 0.37 s, respectively. Fig. 7 shows that the increase in the delay will cause the flow adjustment to fluctuate, resulting in overshoot and the gradual increase of the rotational speed near 0.5 s. Furthermore, the stability time will be prolonged. However, due to the actions of the designed controller, when the rotational speed returns to the rated value, the deviation is less than 0.001, and the time is within 3 s, which meets the requirements of a power grid for frequency change. In addition, the generator power angle is less affected by the change of the delay, and the maximum deviation and the stability time do not fluctuate significantly. These trends suggest that even if the actuator action is delayed, the proposed control method can still enable the relay to control the guide vane to the target position as quickly as possible to realize the power supply frequency and active power output to meet the demands of users.

5.4. Case 4: Disturbance analysis

After the hydroelectric generation set is controlled at a stable operating state, it is necessary to consider a load rejection, a sudden load increase or an accident shutdown of an individual generation system, which may cause a large scale perturbation to other governing systems. Since the frequency directly affects the power quality and the angular speed of the generator rotor determines the power supply frequency, a step excitation with an amplitude of 0.02 is added when the variable runs to 3 s, which represents the frequency fluctuation of the system due to the sudden increase of the load disturbance. As shown in Fig. 8, the relative deviation of the angular speed becomes negative after being disturbed, which is due to the sudden power increase of the generator set; however, the power of the hydroturbine is temporarily unchanged, so the speed of unit decreases. Under the DOBFC, the angular speed amplitude is limited to -0.016, the maximum deviation of the guide vane opening fluctuation is 0.013, and the output is stable at 0.01 after attenuated oscillation; therefore, the generator power angle transits to the response value of 0.02 and remains unchanged. This indicates that the servomotor stroke is temporarily in another controllable state, and the guide vane opening increases to change the flow to rebalance the torque. Therefore, the angular speed can be restored to the rated value in a short time without impacting the power grid. When the system runs to 4 s, the disturbance is removed, the guide vane opening and generator power angle return to the rated conditions, and the speed is stable after a short period of oscillation. Overall, the DOBFC has good immunity to the possible disturbances in the actual rated operations of the fractional-order HTGS.

5.5. Case 5: Effects of parameter variation

The effect of an elastic water hammer on the dynamic performance of the governing system cannot be ignored when the diversion pipeline is long. The maximum value of T_r is set as 3, and the influence on the control performance of the system is studied when the time constant T_r increases from 1 to 3. Fig. 9 shows that the overshoot of the generator power angle

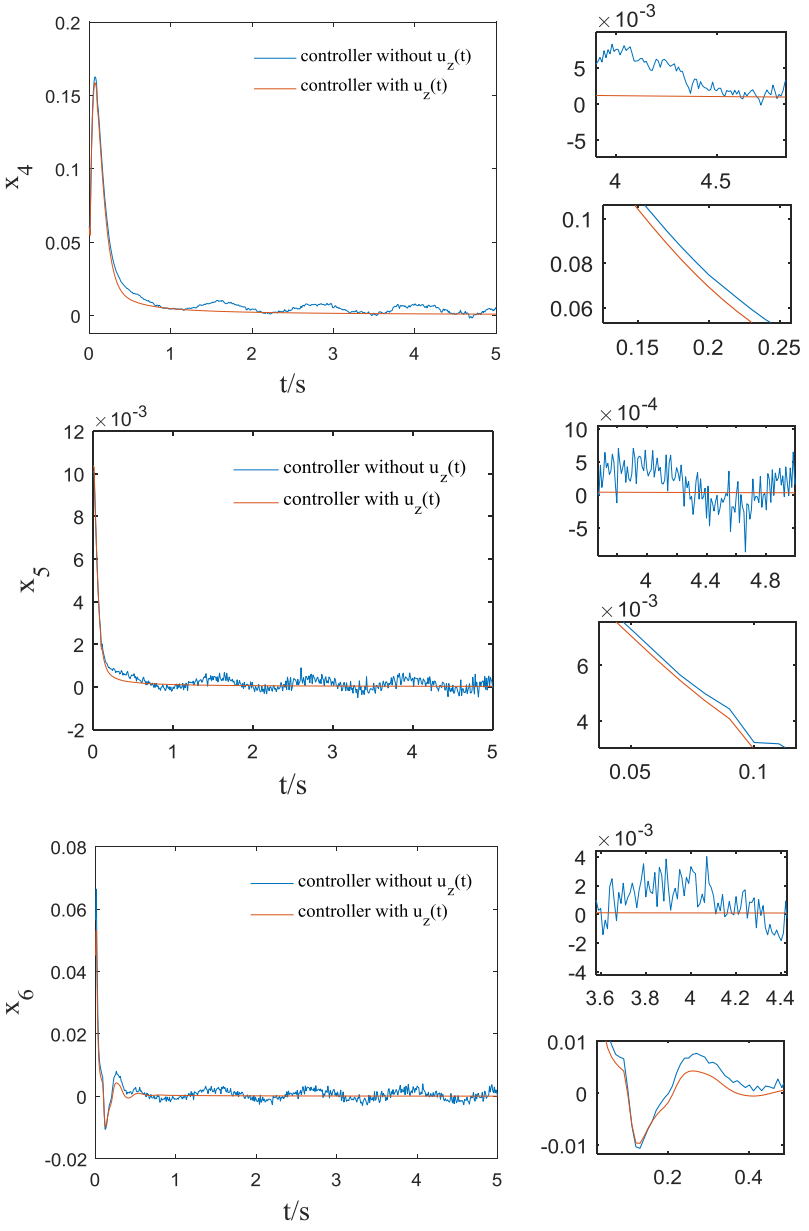

Fig. 4. Control effect comparison of the fuzzy state feedback controller with and without the disturbance suppression function.

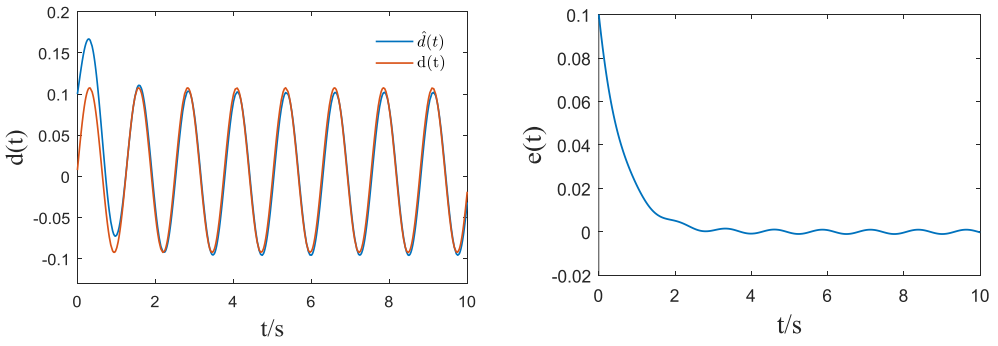

Fig. 5. Disturbance estimated value and error of the controlled fractional-order HTGS.

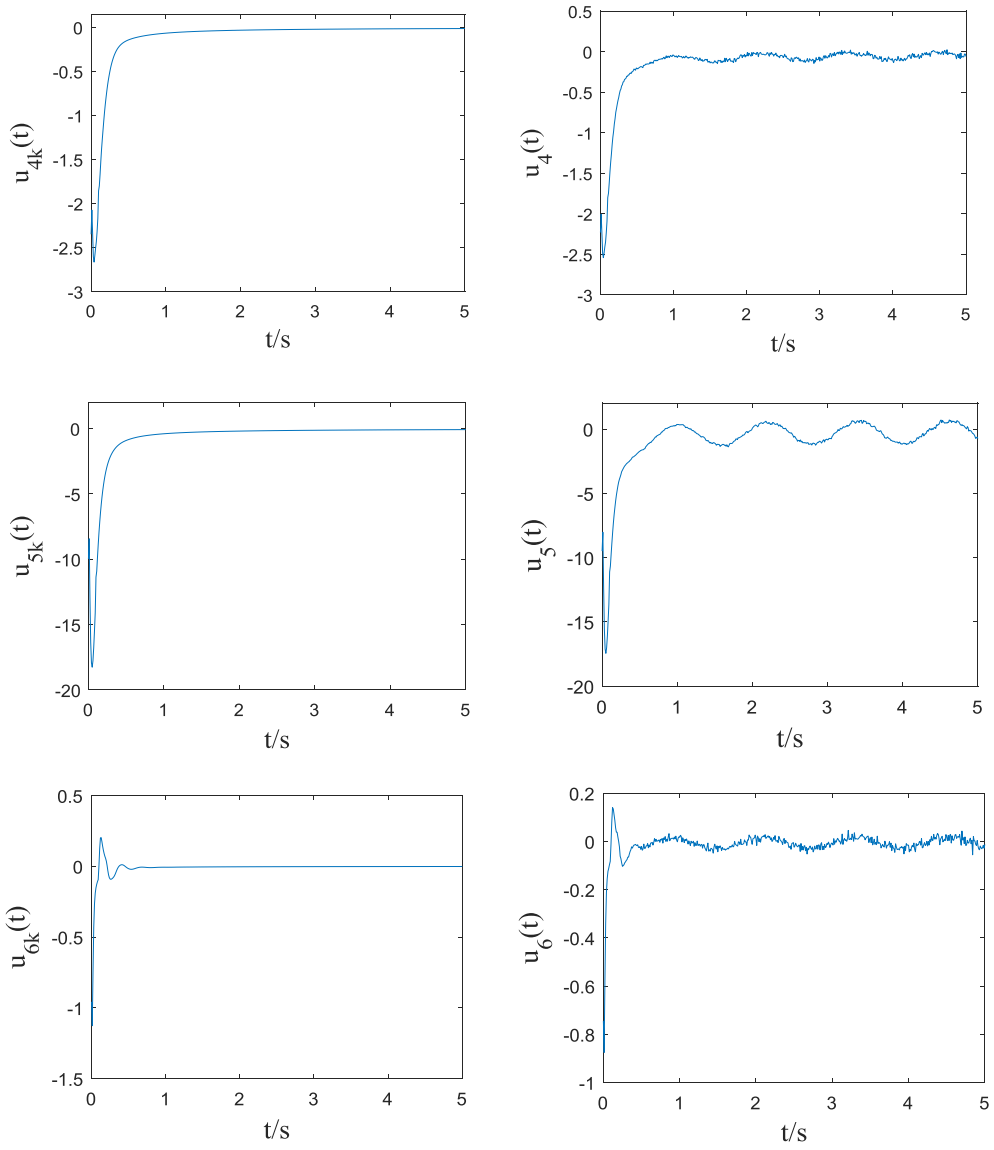

Fig. 6. Output responses of the fuzzy state feedback controller with and without the disturbance suppression function.

increases markedly. When $T_r = 3$, the maximum deviation increases by 40.7%, but under the controller 's action, the angle deviation will descend to the set point fast, and the state trajectories under different T_r can converge rapidly within a small range near zero at 0.5 s; hence, the impact of a water hammer on stabilizing the active power conversion of the unit is reduced. When $T_r = 2.2$, the oscillation peak of the unit speed appears and gradually rises, but the maximum amplitude does not exceed 0.015. Although the stability time has been extended, the steady-state error has met the power demand at 3 s. These features ensure the power supply quality when a water hammer occurs. As shown by the operating curve of the servomotor stroke, the DOBFC can actualize the relay to manipulate the guide vane in accordance with the command under different water hammer effects, and the discrepancies of the oscillation amplitude and transition time are small, which reduces the probability of accidents in the hydraulic system. This shows that DOBFC has good adaptability to complex working conditions and can effectively mitigate the adverse effects of an elastic water hammer on the governing system.

5.6. Case 6: Comparison of the proposed method, PID control and existing method

To further highlight the superiority of the DOBFC applied to the fractional-order HTGS, a comparison is made with the traditional PID control and another fuzzy control method [42] under different orders of the system. The simulation results are given in Fig. 10. And Table 1 is the comparison of transition process performance indicators. By adopting a parallel PID

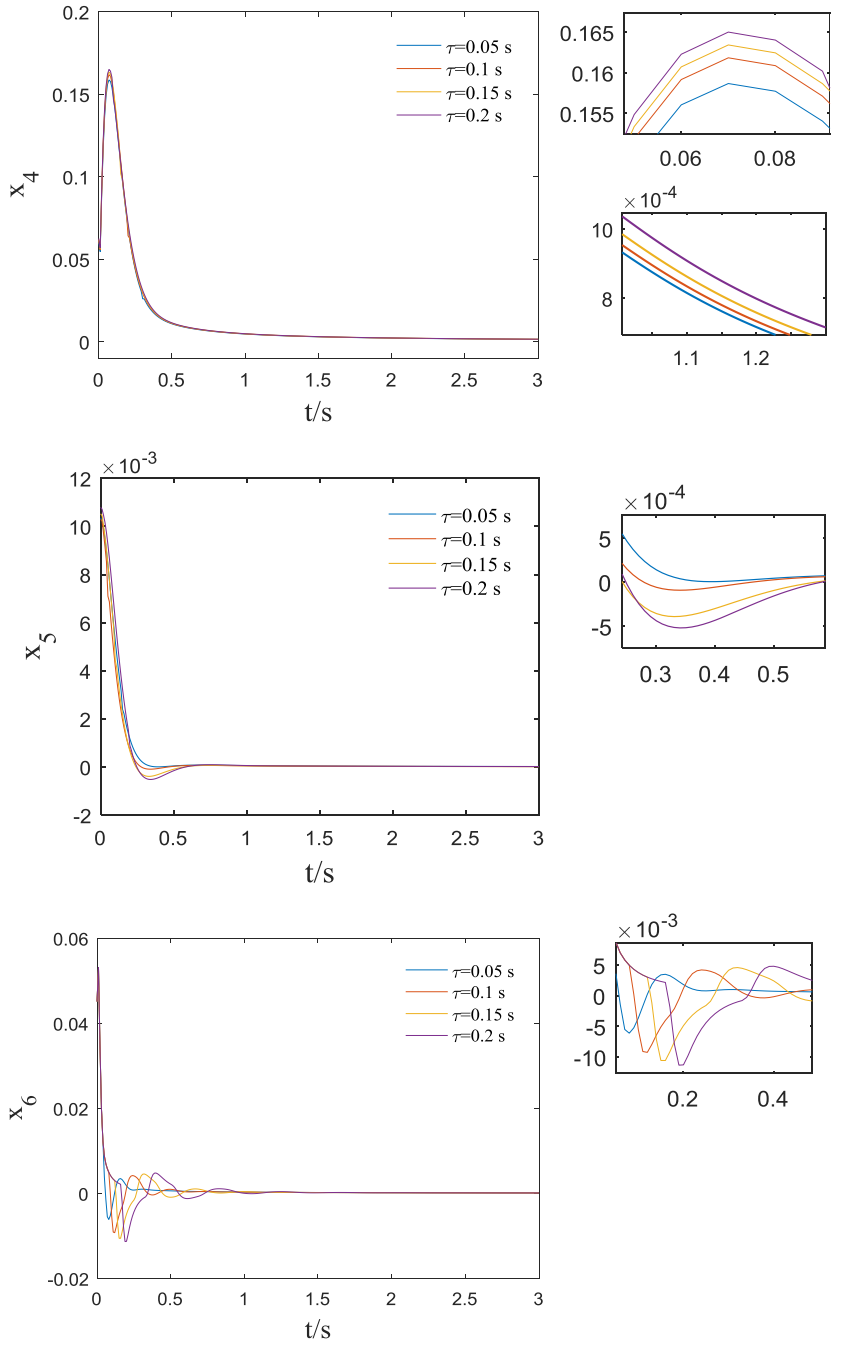

Fig. 7. System responses under four different time delays.

governor as the controller [6,39], the hydraulic servo system in system (6) can be expressed as $T_y D^{\alpha} x_6 + x_6(t-\tau) = U$, where U is the control input and $U = -k_p x_5 - k_d D^{\alpha} x_5 - k_i \frac{x_4}{w_0}$. The control parameters are listed in Tab. 1. According to Ref. [42], system (6) can be considered as a special case where the subsystem and the time-delay item are single. Using the Lyapunov function and the relevant stability analysis in Theorem 1 of [42], the corresponding fuzzy controller can be calculated:

$$\bar{K}_1 = \begin{bmatrix} -0.0000 & 0.0000 & -0.0000 & -32.1402 & 118.3800 & -0.0000 \\ -6.1500 & 0.3481 & -0.5966 & -433.3965 & -31.9394 & -1.3773 \\ 16.0710 & 22.3787 & 13.0733 & 0.0000 & -1.3773 & -120.6824 \end{bmatrix}$$

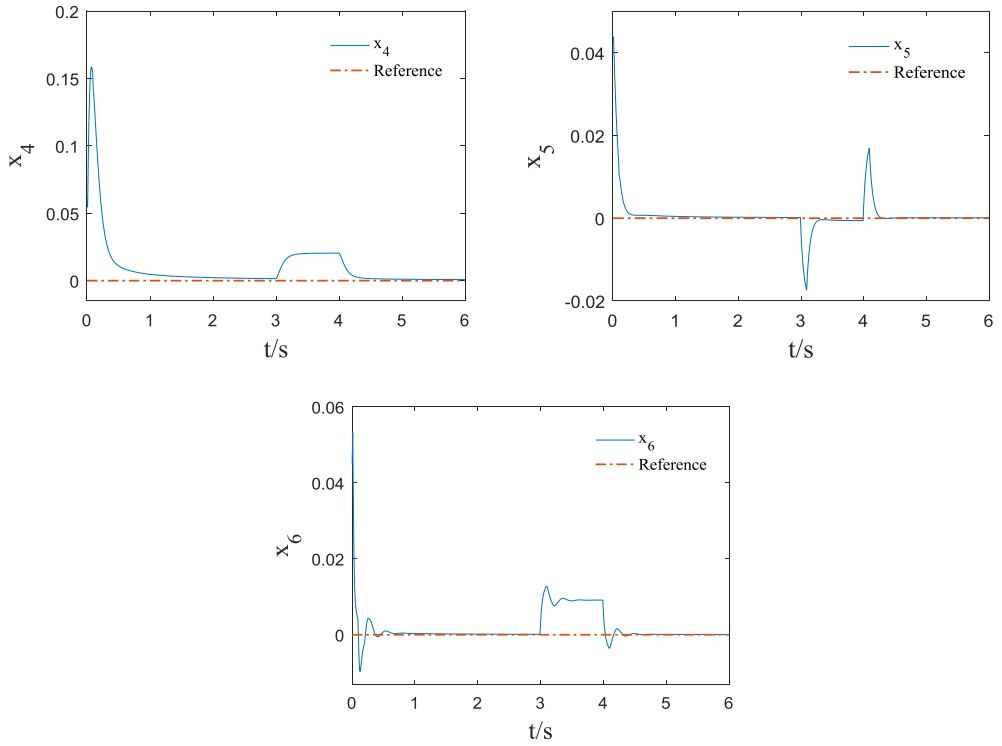

Fig. 8. System responses in the case of a step perturbation effect.

$$\bar{K}_2 = \begin{bmatrix} -0.0000 & 0.0000 & -0.0000 & -32.1402 & -173.3931 & 0.0000 \\ -6.1500 & 0.3481 & -0.5966 & -140.6999 & -31.8374 & -1.3773 \\ 16.0710 & 22.3787 & 13.0387 & -0.0000 & -1.3773 & -120.6824 \end{bmatrix}$$

As shown in Fig. 10, the PID control generally has a long adjustment time and serious oscillation under different orders, and its disadvantage is most obvious when $\alpha = 0.9$. Although α decreases, the degree of oscillation and the duration can be reduced by adjusting the control coefficients, and the control effect is still inferior to the proposed method. The data in Tab. 1 shows that when the system order is from 0.9 to 0.7, the stability time of the state variables under the PID control is shorten by 43.4%, 43% and 43.7%, respectively; and the oscillation frequency of each state decreases. When α ranges from 0.7 to 0.5, the stability time is shorten by 13.8%, 11.6% and 12.7%, respectively; but the number of oscillations does not decrease. Under the existing control method in [42], the stability performance of the HTGS is better than that of the PID control. Although the stability time of the guide vane opening is close to that of the DOBFC method, and even the system can reach the steady state faster when α decreases, the oscillation amplitude is inevitably too large in the transition, which may not meet the actual specified output constraints. In addition, both the power angle and the rotor angular velocity oscillate more times in the transition, resulting in an increase of the stability time. For the DOBFC algorithm, when α ranges from 0.9 to 0.5, the maximum deviations of the system states decrease, and the stability time gradually increases but it is still ahead of that of the PID control. Compared with the method in [42], the DOBFC can shorten the adjustment time of the power angle and the rotor angular velocity by 47.3% and 34.5% respectively, and the transition process is steadier. To summarize, the above analyses prove that the DOBFC is an excellent method worthy of adoption in hydropower systems.

6. Conclusion

For the fractional-order delay HTGS with an external disturbance, the DOBFC method is proposed to suppress the interference. The system model studied can more accurately represent the actual engineering characteristics of hydropower stations. Based on the generalized T-S fuzzy theory, a fractional-order delay fuzzy model was applied to describe the nonlinear system. The disturbance observer is constructed, and the fuzzy state feedback controller is designed to counteract the influence of external disturbances on the system. Furthermore, by virtue of the FDM transformation and Lyapunov methodology, the asymptotic stability criterion for the closed-loop fuzzy system is deduced. The controller parameters are solved by a set of LMIs. Finally, the performed numerical simulation and results analysis highlight that the proposed algorithm ensures that the system has good stability and robustness, even in the presence of disturbances in complex conditions. Compared with

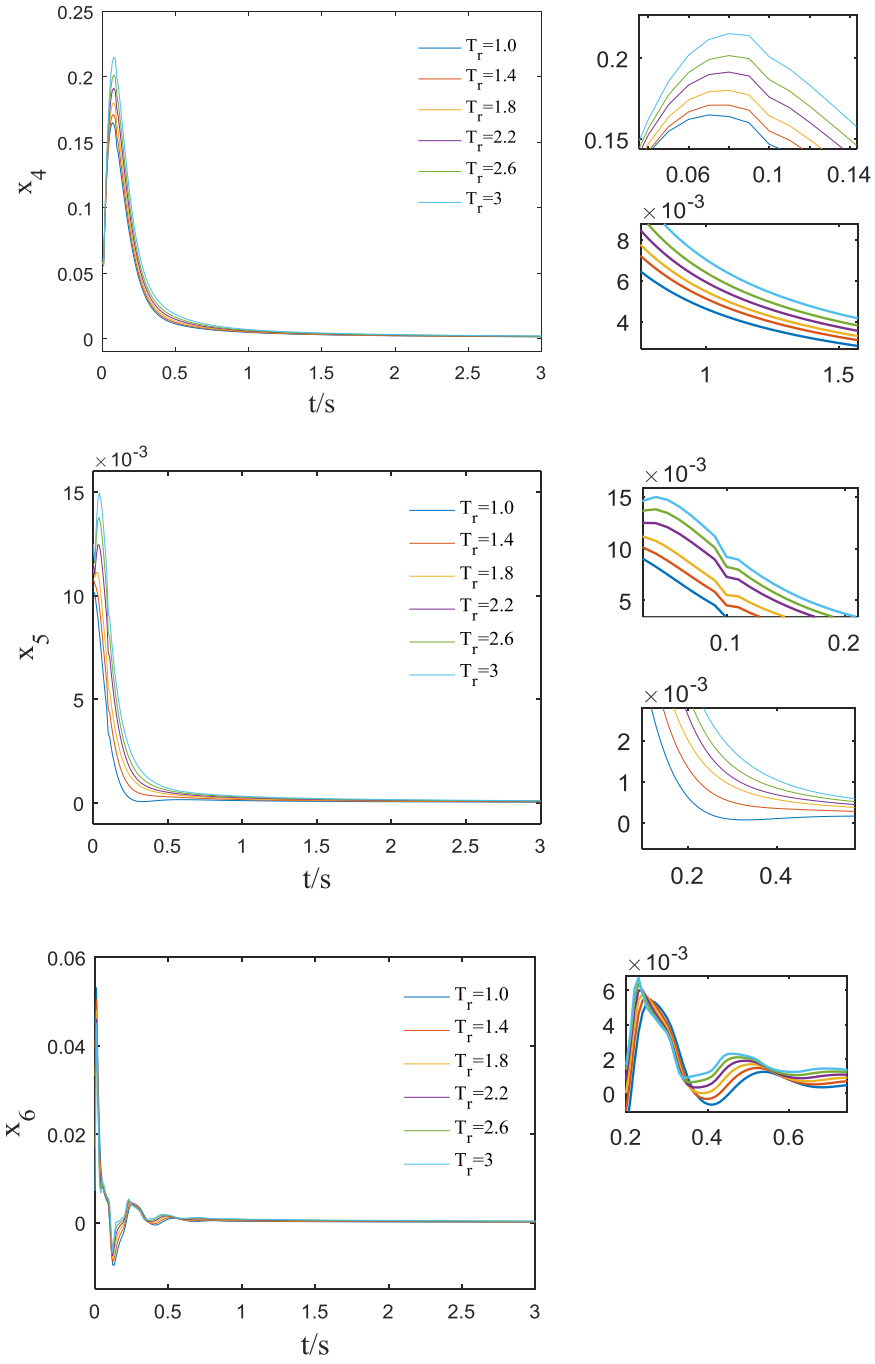

Fig. 9. System responses in the case of parameter variation.

the PID control algorithm and the existing fuzzy control method, the superiority and effectiveness of the new method for different order systems are verified.

The DOBFC method provides a new theoretical reference for the design of HTGS intelligent control algorithm. It has the advantages of small computation, fast response and strong robustness, and is applicable to microcomputer governors. However, it can not keep the optimal control performance for the HTGS with wide range of structure and parameters. In addition, this paper only considers the delay-independent stability criteria, which is more conservative. Therefore, we will further study the fuzzy controller with learning ability to improve its adaptability, and explore the delay-dependent stability analysis method.

Table 1
Comparison of the proposed method, PID control and existing method.

Fractional order		Proposed method		PID control			Existing method	
α	State variable	Maximum deviation	Stability time (s)	Control parameters $k_p k_i k_d$	Maximum deviation	Stability time (s)	Maximum deviation	Stability time (s)
0.9	x_4	0.163	2.2	0.98 0.8 0.5	0.854	8.69	0.163	4.57
	x_5	0.012	1.15		0.012	8.62	0.01	3.27
	x_6	0.053	1.12		0.053	8.61	0.071	1.17
0.8	x_4	0.161	2.26	1.12 0.89 0.6	0.836	7.57	0.163	4.36
	x_5	0.011	1.23		0.012	7.93	0.01	3.25
	x_6	0.053	1.19		0.052	7.35	0.07	1.16
0.7	x_4	0.158	2.31	1.3 1.28 0.9	0.809	4.92	0.162	3.74
	x_5	0.01	1.36		0.011	4.91	0.01	3.18
	x_6	0.051	1.21		0.054	4.85	0.069	1.16
0.6	x_4	0.151	2.35	1.45 1.35 1.12	0.784	4.57	0.161	3.25
	x_5	0.01	1.47		0.01	4.58	0.01	3.17
	x_6	0.047	1.23		0.051	4.56	0.068	1.16
0.5	x_4	0.146	2.41	1.6 1.45 1.23	0.753	4.24	0.158	3.02
	x_5	0.01	1.59		0.01	4.34	0.01	3.17
	x_6	0.046	1.27		0.051	4.23	0.066	1.15

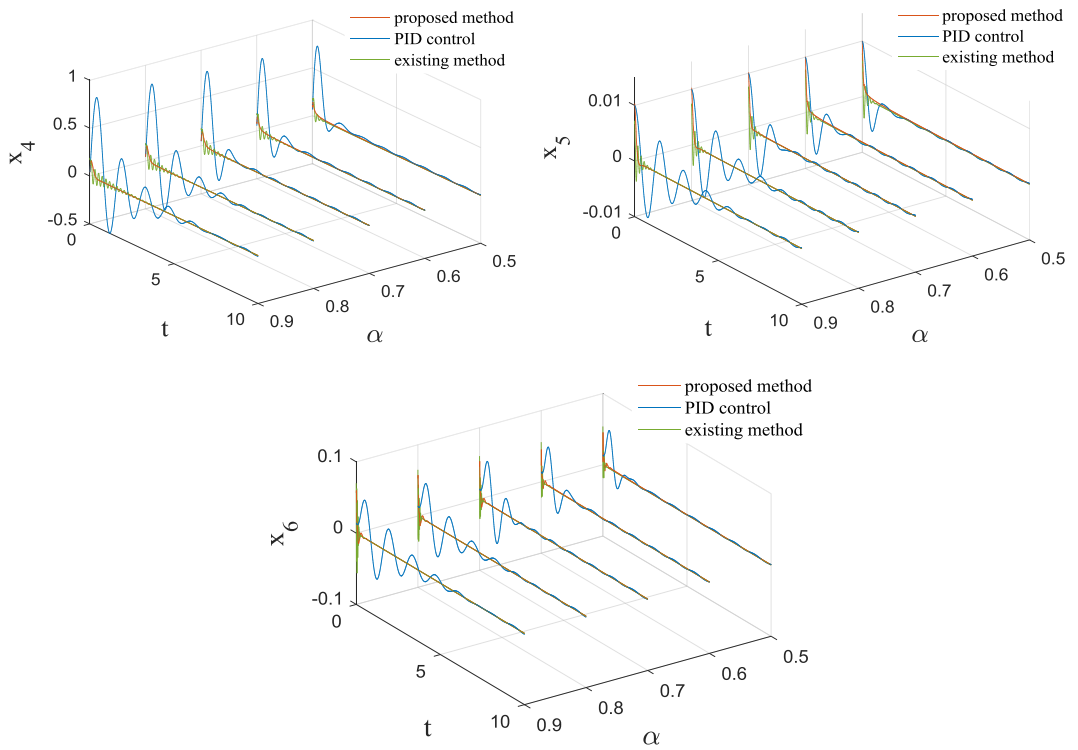

Fig. 10. Control effect comparison when α is 0.9, 0.8, 0.7, 0.6 and 0.5.

CRediT authorship contribution statement

Teng Ma: Investigation, Methodology, Data curation, Software, Validation, Writing - original draft. **Bin Wang:** Conceptualization, Supervision, Writing - review & editing, Project administration, Funding acquisition.

Declaration of Competing Interest

The authors declare that they have no known competing financial interests or personal relationships that could have appeared to influence the work reported in this paper.

Acknowledgements

This work was supported by the scientific research foundation of the Young Scholar Project of Cyrus Tang Foundation, the Shaanxi Province Key Research and Development Plan (Number 2021NY-181) and the National Natural Science Foundation of China (Numbers 51909222 and 51509210).

Appendix A. Supplementary data

Supplementary data to this article can be found online at https://doi.org/10.1016/j.ins.2021.05.013.

References

[1] A. Hussain, G.K. Sarangi, A. Pandit, S. Ishaq, N. Mamnun, B. Ahmad, M.K. Jamil, Hydropower development in the hindu kush Himalayan region: issues, policies and opportunities, Renew. Sust. Energy Rev. 107 (2019) 446–461.
[2] M. Javed, T. Ma, J. Jurasz, M. Amin, Solar and wind power generation systems with pumped hydro storage: review and future perspectives, Renew. Energy 148 (2020) 176–192.
[3] L.N. Proskuryakova, G.V. Ermolenko, The future of Russia's renewable energy sector: trends, scenarios and policies, Renew. Energy 143 (2019) 1670–1686.
[4] C. Li, N. Zhang, X. Lai, J. Zhou, Y. Xu, Design of a fractional-order pid controller for a pumped storage unit using a gravitational search algorithm based on the cauchy and gaussian mutation, Inform. Sci. 396 (2017) 162–181.
[5] X.J. Lai, C.S. Li, W.C. Guo, Y.H. Xu, Y.G. Li, Stability and dynamic characteristics of the nonlinear coupling system of hydropower station and power grid, Commun. Nonlinear Sci. 79 (2019) 104919.
[6] L. Zhang, Q. Wu, Z. Ma, X. Wang, Transient vibration analysis of unit-plant structure for hydropower station in sudden load increasing process, Mech. Syst. Signal Pr. 120 (2019) 486–504.
[7] H. Liu, S. Li, H. Wang, Y. Sun, Adaptive fuzzy control for a class of unknown fractional-order neural networks subject to input nonlinearities and dead-zones, Inform. Sci. 454-455 (2018) 30–45.
[8] J. Qian, Y. Zeng, Y. Guo, L. Zhang, Reconstruction of the complete characteristics of the hydro turbine based on inner energy loss, Nonlinear Dyn. 86 (2) (2016) 963–974.
[9] P. Mani, R. Rajan, L. Shanmugam, Y. Hoon Joo, Adaptive control for fractional order induced chaotic fuzzy cellular neural networks and its application to image encryption, Inform. Sci. 491 (2019) 74–89.
[10] J. Zhao, J. Wang, S. Wang, Fractional order control to the electro-hydraulic system in insulator fatigue test device, Mechatronics 23 (7) (2013) 828–839.
[11] P. Pennacchi, S. Chatterton, A. Vania, Modeling of the dynamic response of a Francis turbine, Mech. Syst. Signal Pr. 29 (2012) 107–119.
[12] F.J. Wu, F. Li, P. Chen, B. Wang, Finite-time control for a fractional-order nonlinear hydro-turbine governing system, IET Renew. Power Gen. 13 (2019) 633–639.
[13] Y. Zheng, J. Zhou, W. Zhu, C. Zhang, C. Li, W. Fu, Design of a multi-mode intelligent model predictive control strategy for hydroelectric generating unit, Neurocomputing 207 (2016) 287–299.
[14] J. Xiao, J. Cao, J. Cheng, S. Zhong, S. Wen, Novel methods to finite-time mittag-leffler synchronization problem of fractional-order quaternion-valued neural networks, Inform. Sci. 526 (2020) 221–244.
[15] Y. Li, Y.Q. Chen, I. Podlubny, Stability of fractional-order nonlinear dynamic systems: Lyapunov direct method and generalized Mittag-Leffler stability, Comput. Math. Appl. 59 (2010) 1810–1821.
[16] Z. Yang, S. Zheng, F. Liu, Y. Xie, Adaptive output feedback control for fractional-order multi-agent systems, ISA Trans. 96 (2020) 195–209.
[17] H. Dai, W. Chen, New power law inequalities for fractional derivative and stability analysis of fractional order systems, Nonlinear Dyn. 87 (3) (2017) 1531–1542.
[18] R.-E. Precup, S. Preitl, Development of fuzzy controllers with non-homogeneous dynamics for integral-type plants, Electr Eng. 85 (3) (2003) 155–168.
[19] S.-K. Oh, W.-D. Kim, W. Pedrycz, Design of optimized cascade fuzzy controller based on differential evolution: simulation studies and practical insights, Eng. Appl. Artif. Intel. 25 (3) (2012) 520–532.
[20] R.-E. Precup, M.L. Tomescu, Stable fuzzy logic control of a general class of chaotic systems, Neural Comput. Appl. 26 (3) (2015) 541–550.
[21] H.N. Wu, J.W. Wang, H.X. Li, Design of distributed H-infinity fuzzy controllers with constraint for nonlinear hyperbolic PDE systems, Automatica 48 (2012) 2535–2543.
[22] D. Chen, R. Zhang, X. Liu, X. Ma, Fractional order Lyapunov stability theorem and its applications in synchronization of complex dynamical networks, Commun. Nonlinear Sci. 19 (12) (2014) 4105–4121.
[23] S. Song, B. Zhang, J. Xia, Z. Zhang, Adaptive backstepping hybrid fuzzy sliding mode control for uncertain fractional-order nonlinear systems based on finite-time scheme, IEEE Trans. Syst. Man Cy-S. 50 (4) (2020) 1559–1569.
[24] B. Wang, J. Xue, F. Wu, D. Zhu, Robust Takagi-Sugeno fuzzy control for fractional order hydro-turbine governing system, ISA Trans. 65 (2016) 72–80.
[25] K. Shi, B. Wang, H. Chen, Fuzzy generalized predictive control for a fractional-order nonlinear hydro-turbine regulating system, IET Renew. Power Gen. 12 (2018) 1708–1713.
[26] J. Kluska, Adaptive fuzzy control of state-feedback time-delay systems with uncertain parameters, Inform. Sci. 540 (2020) 202–220.
[27] H. Liu, X.Z. Lin, Finite-time H-infinity control for a class of nonlinear system with time-varying delay, Neurocomputing 149 (2015) 1481–1489.
[28] T. Haidegger, L. Kovács, R.-E. Precup, S. Preitl, B. Benyó, Z. Benyó, Cascade control for telerobotic systems serving space medicine, IFAC Proc. 44 (1) (2011) 3759–3764.
[29] A. Turnip, J.H. Panggabean, Hybrid controller design based magneto-rheological damper lookup table for quarter car suspension, Int. J. Artif. Intell. 18 (2020) 193–206.
[30] B. Xu, F. Wang, D. Chen, H. Zhang, Hamiltonian modeling of multi-hydro-turbine governing systems with sharing common penstock and dynamic analyses under shock load, Energy Convers. Manage. 108 (2016) 478–487.
[31] S. Huang, L. Xiong, J. Wang, P. Li, Z. Wang, M. Ma, Fixed-time synergetic controller for stabilization of hydraulic turbine regulating system, Renew. Energy 157 (2020) 1233–1242.
[32] S. Simani, S. Alvisi, M. Venturini, Fault tolerant control of a simulated hydroelectric system, Control Eng. Pract. 51 (2016) 13–25.
[33] B. Wang, X. Yu, L. Mu, Y. Zhang, Disturbance observer-based adaptive fault-tolerant control for a quadrotor helicopter subject to parametric uncertainties and external disturbances, Mech. Syst. Signal Pr. 120 (2019) 727–743.
[34] J. Wang, C. Shao, Y.-Q. Chen, Fractional order sliding mode control via disturbance observer for a class of fractional order systems with mismatched disturbance, Mechatronics 53 (2018) 8–19.
[35] M. Chen, S.Y. Shao, P. Shi, Y. Shi, Disturbance-observer-based robust synchronization control for a class of fractional-order chaotic systems, IEEE Trans. Circuits II (64) (2017) 417–421.
[36] R. Almeida, A Caputo fractional derivative of a function with respect to another function, Commun. Nonlinear Sci. 44 (2017) 460–481.
[37] J.C. Trigeassou, N. Maamri, J. Sabatier, A. Oustaloup, State variables and transients of fractional order differential systems, Comput. Math. Appl. 64 (10) (2012) 3117–3140.

[38] J. Maryska, M. Rozložník, M. Tuma, Schur complement systems in the mixed-hybrid finite element approximation of the potential fluid flow problem, Siam J. Sci. Comput. 22 (2) (2000) 704–723.
[39] B. Xu, D. Chen, H. Zhang, F. Wang, Modeling and stability analysis of a fractional-order francis hydro-turbine governing system, Chaos Soliton. Fract. 75 (2015) 50–61.
[40] L.-D. Zhao, J.-B. Hu, J.-A. Fang, W.-B. Zhang, Studying on the stability of fractional-order nonlinear system, Nonlinear Dynam. 70 (1) (2012) 475–479.
[41] T.A. Burton, Fractional differential equations and Lyapunov functionals, Nonlinear Anal-Theor. 74 (16) (2011) 5648–5662.
[42] Y. Li, J. Li, Decentralized stabilization of fractional order T-S fuzzy interconnected systems with multiple time delays, J. Intell. Fuzzy Syst. 30 (1) (2015) 319–331.